Ferromagnetism, superconductivity and quantum criticality in uranium intermetallics

Nguyen Thanh, H.

Publication date
2008

5. Ferromagnetic quantum critical point in single-crystalline $URh_{0.62}Ru_{0.38}Ge$

5.1. Introduction

In Chapter 4 we have reported the evolution of ferromagnetism of the polycrystalline $URh_{1-x}Ru_xGe$ series. Upon Ru doping ferromagnetism is smoothly suppressed and vanishes at the FM QCP $x_{cr} = 0.38$. Non-Fermi Liquid (NFL) behaviour is observed for samples with Ru concentration near x_{cr}. This offers a rare opportunity to study FM spin fluctuations near a ferromagnetic quantum critical point at ambient pressure. However, such a study preferably should be carried out on single-crystalline samples, as one expects a strong magneto-crystalline anisotropy for the orthorhombic TiNiSi structure [40]. Especially, inelastic neutron scattering studies to probe the critical fluctuations require large high-quality single-crystals.

In this chapter, we report the first investigations of a single-crystalline sample $URh_{1-x}Ru_xGe$ with x near the critical concentration $x_{cr} \approx 0.38$. Transport, magnetization and specific-heat measurements in high magnetic fields have been carried out. The data reveals a strong anisotropy of the easy-plane type, with the a-axis as the hard axis. Upon applying a magnetic field our sample is tuned away from the FM QCP and the Fermi liquid state is recovered.

5.2. Sample preparation and characterization

A polycrystalline batch with nominal composition $U_{1.01}Rh_{0.62}Ru_{0.38}Ge$ was prepared by

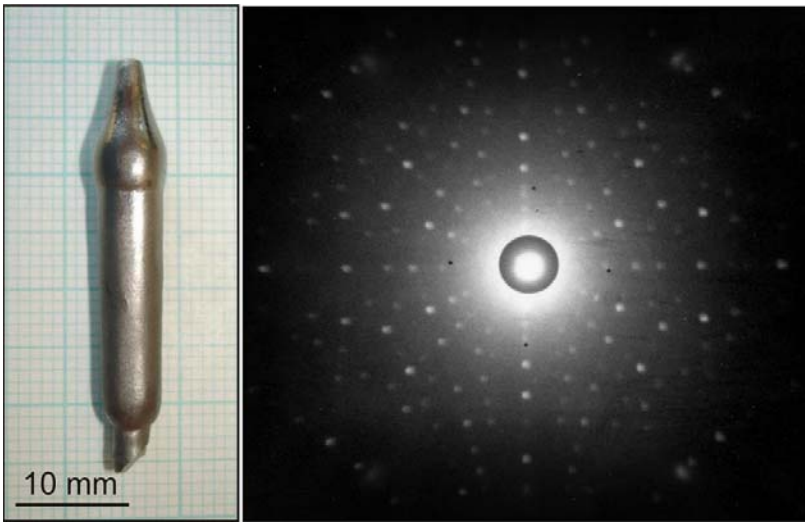

Figure 5.1 X-ray Laue picture (*right panel*) of as-grown single crystalline $URh_{0.62}Ru_{0.38}Ge$ (*left panel*).

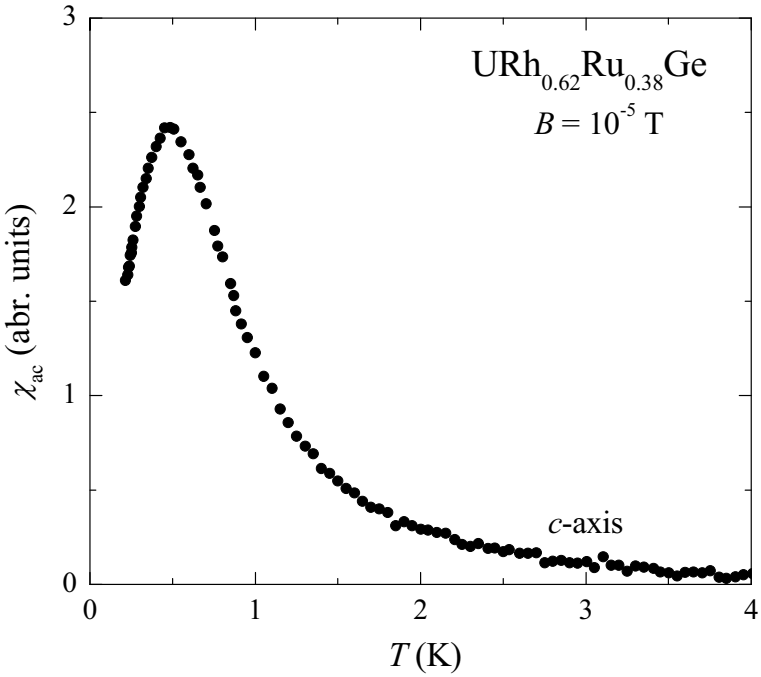

Figure 5.2 Temperature dependence of the ac-susceptibility for the $URh_{0.62}Ru_{0.38}Ge$ crystal measured at a low frequency of 16 Hz and in a small driving field of ~ 10^{-5} T applied along the *c*-axis (data taken by A. Gasparini [145]).

arc-melting the constituents (natural U 3N, Rh 3N, Ru 3N and Ge 5N) in a water-cooled copper crucible under a high-purity argon atmosphere. The polycrystalline ingot was used as a seed for the single-crystal, grown by a modified Czochralski method in a tri-arc furnace under a high-purity argon atmosphere. No subsequent heat treatment was given to the single-crystal. In Fig. 5.1 we show a picture and Laue pattern of the single-crystal,

which is 5 - 6 mm in diameter and 35 mm in length. EPMA analysis confirmed that the crystal is single-phase and homogeneous. Single-crystallinity was checked by X-ray Laue backscattering. Samples for various measurements were cut by spark erosion.

Ac-susceptibility measurements carried out on a small piece of the crystal [145] show a weak ordering peak at a temperature around 0.4 K, see Fig. 5.2. This indicates that the single-crystal orders ferromagnetically at a Curie temperature $T_C \approx 0.4$ K and that $x < x_{cr}$. When comparing with $T_C(x)$ obtained for the polycrystalline samples (see Fig. 4.17), we conclude that $T_C = 0.4$ K corresponds to $x = 0.375$. Thus the actual Ru content in the single-crystal appears to be slightly lower the nominal value $x = 0.38$. As mentioned in Section 4.2, we cannot determine the exact atomic ratio of Rh and Ru using the EPMA technique, and in the following we use the nominal value $x = 0.38$.

5.3. Electrical resistivity

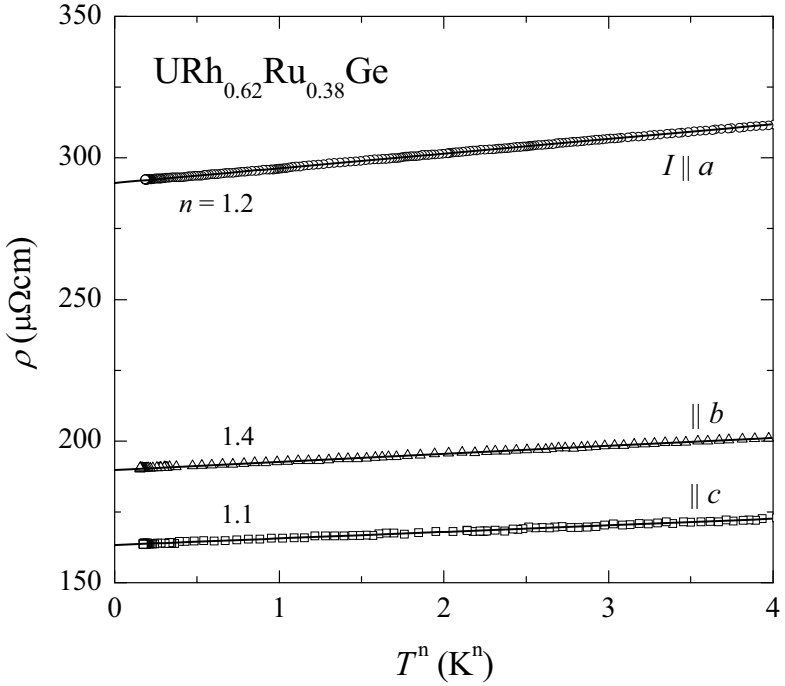

Figure 5.3 The resistivity of single-crystalline $URh_{0.62}Ru_{0.38}Ge$ plotted versus T^n for a current along the principal axes, as indicated. The solid lines represent fits of the data to $\rho \sim T^n$.

In Fig. 5.3, we show the temperature variation of the resistivity of the $URh_{0.62}Ru_{0.38}Ge$ single-crystal plotted as ρ versus T^n for the current I along the principal axes. The overall resistivity values for $I \parallel a$ are about a factor 3/2 larger for $I \parallel b$ and $I \parallel c$. The residual

resistance ratio's (*RRR*) are quite low and amount to ~ 2. By fitting the data to $\rho \sim T^n$ in the temperature range 0.25 - 4 K, we extract values for the exponent n of 1.2, 1.4 and 1.1 for $I \parallel a$, b and c, respectively. These n exponents are close to the value $n \approx 1.2$ obtained for polycrystalline $URh_{1-x}Ru_xGe$ with $x \sim 0.38$ (see Fig. 4.12). We conclude the non-Fermi liquid (NFL) behaviour locates our sample close to the FM QCP. In Table 5.1, we summarize the fit-parameters from the transport data.

For polycrystalline $URh_{0.62}Ru_{0.38}Ge$, resistivity measurements in magnetic fields demonstrated that the FL state is recovered upon field application of the magnetic field. The effect of a magnetic field on the resistivity of the single-crystalline samples has not been investigated yet.

Table 5.1 The parameters ρ_0, n and A obtained by fitting the resistivity to $\rho = \rho_0 + AT^n$ (Eq. 4.5) for the $URh_{0.62}Ru_{0.38}Ge$ crystal.

I direction	ρ_0 (μΩcm)	n	A (μΩcm/K^n)
a-axis	291	1.2	5.19
b-axis	190	1.4	2.80
c-axis	163	1.1	2.31

5.4. Magnetic properties

The field dependence of the magnetization of the $URh_{0.62}Ru_{0.38}Ge$ single-crystal, measured in magnetic fields up to 50 T applied along the principal axes at T = 4.2 K, is shown in Fig. 5.4. The magnetization M is strongly anisotropic. The induced moment initially grows fastest for B along the c-axis, but for $B > 27$ T $M_b > M_c$. The magnetic anisotropy is of the easy-plane type, with the a-axis being the hard axis. For $B \parallel a$, the magnetization linearly increases up to the highest field. The anisotropy in the magnetization of doped URhGe mimics the anisotropy observed for pure URhGe, where a spin reorientation process takes place in the bc-plane for a field of 12 T directed along the b-axis. The induced moment in the bc-plane near 50 T amount to 0.6 μ_B, which is still much smaller than the saturation values M_S = 3.58 or 3.62 μ_B for the $5f^2$ and $5f^3$ configurations. We did not observe a positive curvature of dM/dB that could hint at a spin-reorientation, or a re-entrant FM transition, predicted for a compound located in the vicinity of a ferromagnetic quantum critical end-point [89].

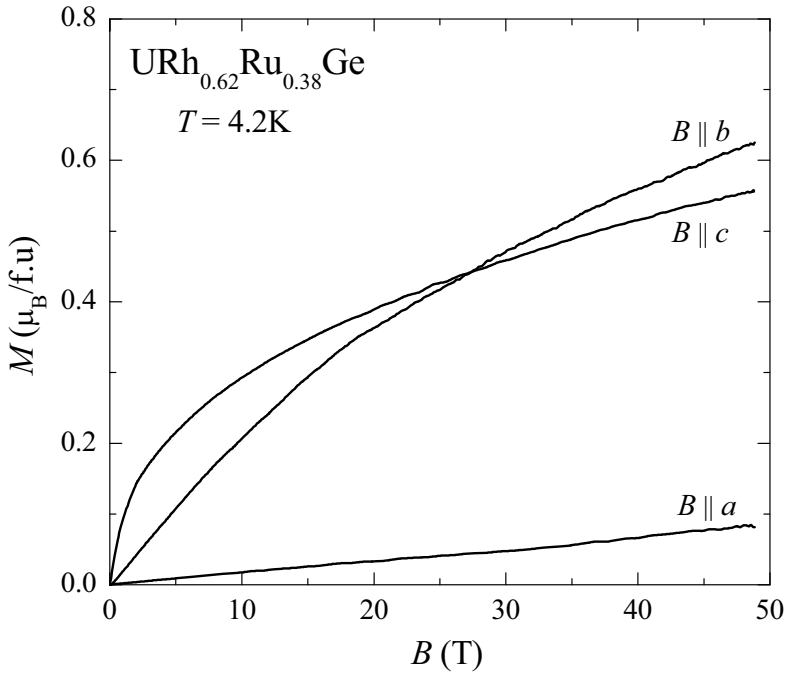

Figure 5.4 The high-field magnetization of single-crystalline $URh_{0.62}Ru_{0.38}Ge$ measured in a field up to 50 T applied along the principal axes as indicated, at $T = 4.2$ K.

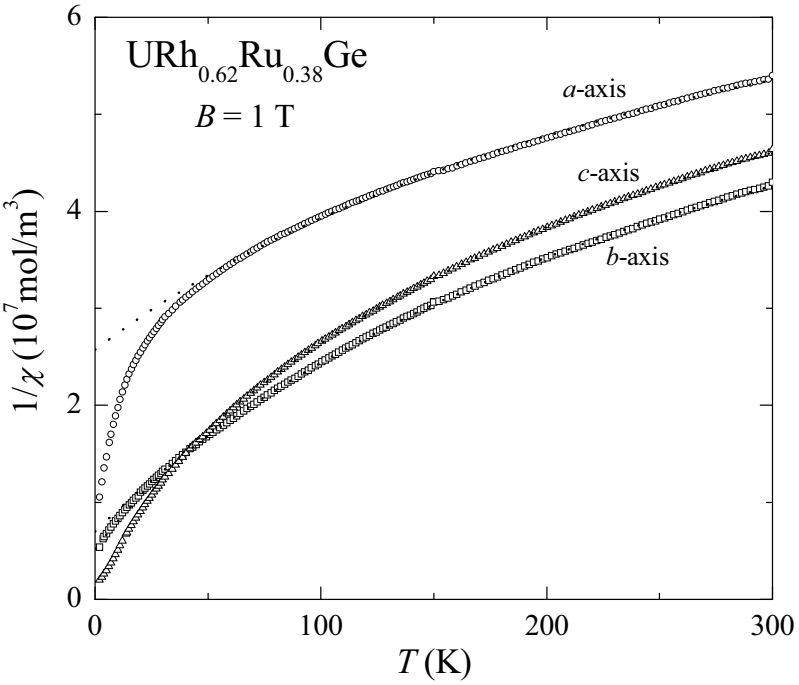

Figure 5.5 Temperature variation of the reciprocal susceptibility of the $URh_{0.62}Ru_{0.38}Ge$ single-crystal measured in a field of 1 T applied along the principal axes. The dotted lines are the best fits to a MCW law in the temperature range 50 - 300 K.

The reciprocal susceptibility of the single-crystalline $URh_{0.62}Ru_{0.38}Ge$ sample measured in a field $B = 1$ T applied along the *a*-, *b*- and *c*-axis in the temperature range 2 - 300 K is shown in Fig. 5.5. Above 50 K the magnetic susceptibility follows a MCW law with

$\chi_0 \sim 10^{-8}$ m^3/mol. The data confirm a magnetic anisotropy, of the easy-plane type with the hard-magnetization direction along the *a*-axis. This is also reflected in the paramagnetic Curie temperature $\theta_a \gg \theta_b, \theta_c$. The values of the effective moment p_{eff} listed in Table 5.2 indicate that the largest moment is induced for $B \parallel b$ in the paramagnetic region ($T > 50$ K). This is in good agreement with the susceptibility data reported on single-crystalline URhGe [119].

Table 5.2 The effective moment p_{eff} and the paramagnetic Curie temperature θ of the $URh_{0.62}Ru_{0.38}Ge$ single-crystal as deduced from magnetization measurements.

B direction	p_{eff} (μ_B/f.u.)	θ (K)
a-axis	1.32	-101.5
b-axis	1.53	-28.1
c-axis	1.38	-16.6

5.5. Specific heat

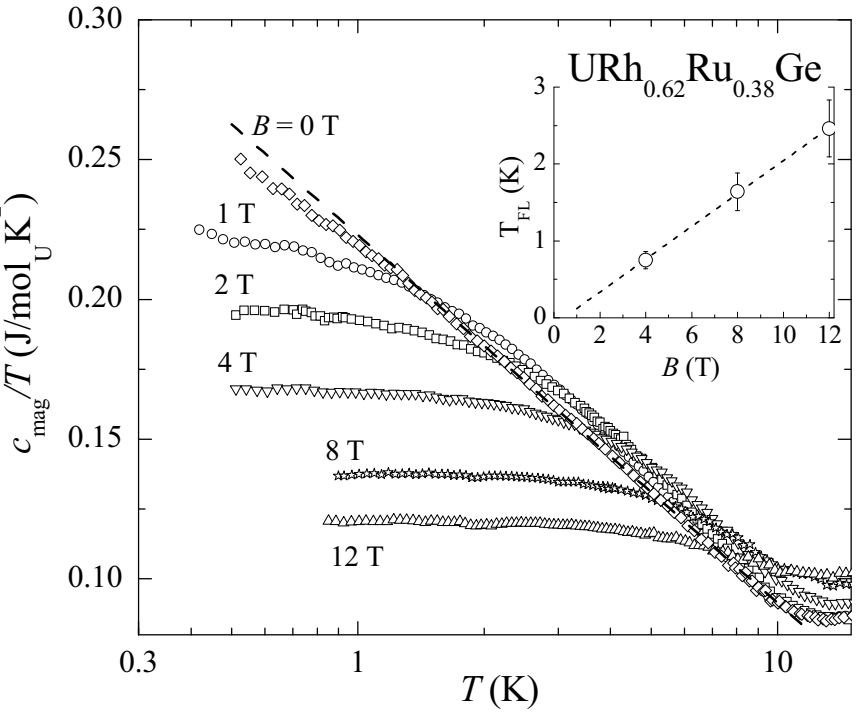

Figure 5.6 f-electron specific heat of single-crystalline $URh_{0.62}Ru_{0.38}Ge$ plotted as c_{mag}/T versus T (on a logarithmic scale) in magnetic fields of 0, 1, 2, 4, 8 and 12 T applied along the easy axis *c*. The dashed line represents a fit $c_{mag}/T = -b\ln(T/T_0)$ (Eq. 4.9) with $b = 0.057$ J/molK^2 and the scaling temperature $T_0 = 49.5$ K for the data measured in zero field. *Inset*: the field-dependence of T_{FL}.

Specific heat measurements on the $URh_{0.62}Ru_{0.38}Ge$ crystal are performed in magnetic fields up to 12 T in the temperature interval 0.5 - 20 K. The magnetic field was directed along the *c*-axis, *i.e.* the easy direction for magnetization, in order to induce the largest effect. The lattice contribution to the specific heat, $c_{lat} = \beta T^3$, is obtained by fitting the data measured in zero field in the temperature range 10 K < T < 20 K. We find $\beta = 0.60\times10^{-3}$ J/molK^4 and $\theta_D \approx 210$ K which are the same values as obtained for the polycrystalline samples (see Section 4.5).

In Fig. 5.6, we show the *f*-electron specific heat divided by temperature c_{mag}/T, obtained after subtracting the lattice contribution, in different fields. Here the data are plotted on a logarithmic temperature scale.

The zero-field data show pronounced NFL behaviour. Below 10 K c_{mag}/T grows in a (quasi)logarithmic fashion down to 2 K: $c_{mag}/T = -b\ln(T/T_0)$ with $b = 0.057$ J/molK^2 and the scaling temperature $T_0 = 49.5$ K. The values for b and T_0 are almost identical to the values obtained for the polycrystalline sample at the critical concentration $x_{cr} = 0.38$. However, below 2 K the data deviate from the ln$T$ behaviour, because for the single-crystal $x < x_{cr}$ and magnetic order sets in at ~ 0.4 K (see Fig. 5.2)

In a magnetic field applied along the *c*-axis, c/T is suppressed and levels off towards a constants value for $T \rightarrow 0$. This shows the FL state is recovered in a field. The characteristic temperature T_{FL}, at which c/T becomes constant, increases with magnetic field, as shown in the inset of Fig. 5.6. By linearly fitting the $T_{FL}(B)$ data, we extract a small value $T_{FL} \approx 0.2$ K when $B \rightarrow 0$. This reveals the single-crystal is located close to the QCP. In the temperature range $T > 10$ K the magnetic contribution to the specific heat increases with applied fields, see Fig. 5.6. This shows entropy is transferred from low to high temperatures.

The c/T values measured at 0.5 K decrease gradually with magnetic fields. $c/T(B)$ follows an exponential decay function [119] (see the left panel of Fig. 5.7)

$$c/T\big|_{0.5K}(H) = c/T\big|_{0.5K}(\infty) + A(1 - e^{-\mu_0 H/\Delta_B}) \qquad (5.1)$$

Here $c/T|_{0.5K}(\infty) = 0.113$ J/molK^2 represents the value of $c/T|_{0.5K}$ for $B \rightarrow \infty$, $\Delta_B = 4.23$ T describes how fast $c/T|_{0.5K}$ decays with increasing field, and $A = 0.136$ J/molK^2 is a fitting parameter.

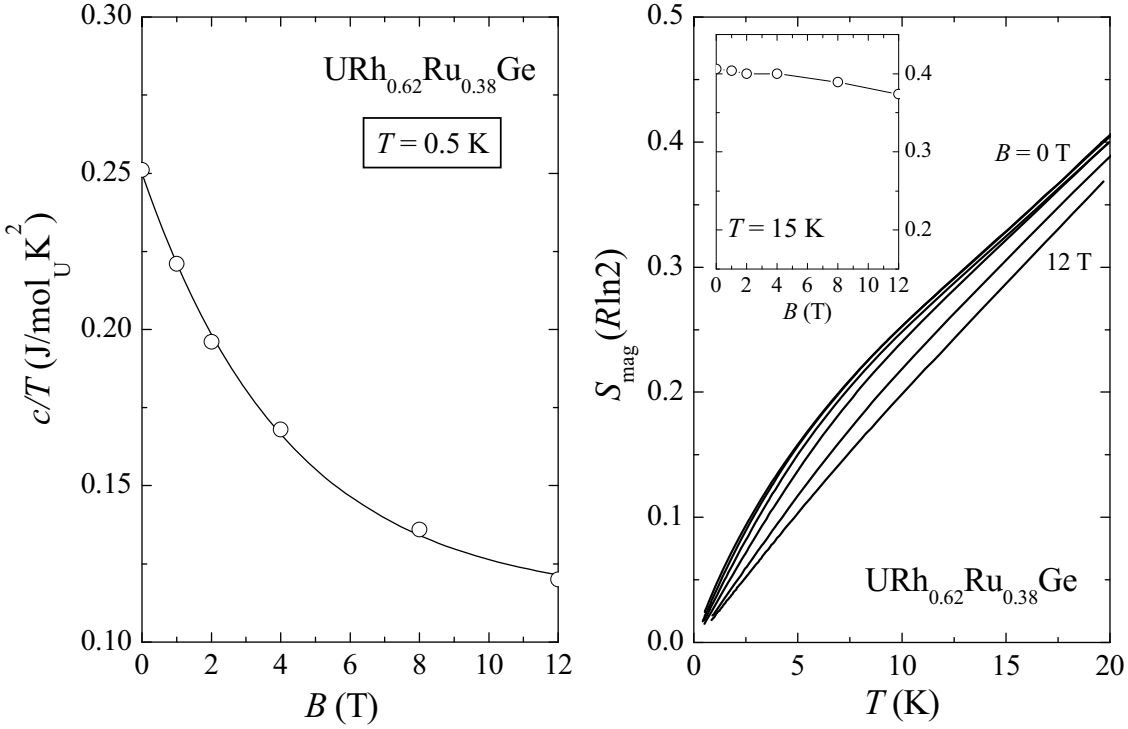

Figure 5.7 Left panel: The γ value (c/T value at 0.5 K or extrapolated for B = 8 and 12 T) as a function of magnetic field B. *Right panel*: The magnetic entropy S_{mag} (in units of Rln2) for the $URh_{0.62}Ru_{0.38}Ge$ single-crystal. The applied fields are (from top to bottom) B = 0, 1, 2, 4, 8 and 12 T. *Inset*: The field-dependence of S_{mag} at a fixed temperature of 15 K.

The magnetic entropy S_{mag}, which is calculated by integrating c_{mag}/T versus T between 0.5 and 15 K is shown in the right panel of Fig. 5.7. In zero field, S_{mag} is about 0.33Rln2 which is in good agreement with the value obtained on the polycrystalline sample with x = 0.38. Upon applying a magnetic field, S_{mag} slightly decreases to a value 0.29Rln2 for B = 12 T.

5.6. Discussion

The transport and magnetization data of single-crystalline $URh_{0.62}Ru_{0.38}Ge$ reveal strong magnetocrystalline anisotropy of the easy-plane type, with the hard-magnetization direction along the *a*-axis. This anisotropy reflects the one in pure URhGe. URhGe is a uniaxial ferromagnet with the magnetic moment along the orthorhombic *c*-axis [36]. However, upon application of a magnetic field along the *b*-axis the moment rotates in the *bc*-plane toward the *b*-axis, while the *a*-axis is the hard axis [38]. The strong magnetocrystalline anisotropy stresses the need to carry out all subsequent experiments, like neutron scattering to probe the anisotropic spin-fluctuation spectrum, on single-crystalline samples.

Upon application of a magnetic field $B \parallel c$, the FL state is recovered. Evidence for this is provided by the suppression of the specific heat, notably the levelling off towards constant values of c/T for $T \rightarrow 0$. A similar behaviour has been observed in other NFL doped-systems [146-148]. However, the only other FM case is the $CePd_{1-x}Rh_x$ series [148]. Experiments on polycrystalline samples show that $CePd_{1-x}Rh_x$ exhibits a "smeared" FM QCP at $x_{cr} = 0.87$ [27]. The NFL behaviour observed near $x_{cr} = 0.87$ is then a consequence of the distribution of single-ion Kondo temperatures, and can be explained by the Kondo disorder model [149]. Also, the c_{mag}/T versus T data of $CePd_{1-x}Rh_x$ for $x \sim x_{cr}$ develop a broad maximum at a characteristic temperature T_{max} upon applying a magnetic field [148]. T_{max} increases linearly with increasing magnetic field and attains a value of ~ 1 K for a field $B = 3$ T. The field-induced broad maximum is tentatively attributed to a Schottky anomaly connected with the Zeeman splitting of the partially Kondo-screened crystal-electric-field ground-state doublet in the external magnetic field [150]. A similar phenomenon, *i.e.*, a maximum in c_{mag}/T versus T, is not observed in the specific heat data of the $URh_{0.62}Ru_{0.38}Ge$ single-crystal: c_{mag}/T tends to level off and saturates in the limit $T \rightarrow 0$ for fields up to 12 T. The difference in behaviour can be attributed to the very different scaling temperatures T_0 deduced from the $c_{mag}/T = -b\ln(T/T_0)$ behaviour. For $URh_{0.62}Ru_{0.38}Ge$ $T_0 \approx 50$ K, while for $CePd_{0.13}Rh_{0.87}$ $T_0 \approx 5.5$ K. This shows the NFL behaviour is more robust in $URh_{0.62}Ru_{0.38}Ge$ and fields much larger than 12 T are needed to resolve the Zeeman splitting.

In conclusion, we have presented the first study of the FM QCP in a single crystal of $URh_{0.62}Ru_{0.38}Ge$. The results show a strong magnetocrystalline anisotropy of the easy-(*bc*) plane type, with the *a*-axis as the hard-magnetization direction. Specific-heat data in a magnetic field ($B_{max} = 12$ T) applied along the *c*-axis show that $URh_{0.62}Ru_{0.38}Ge$ can be tuned away from the FM QCP and that the Fermi liquid state is recovered. In order to learn more about the anisotropic nature of the break-down of the NFL behaviour near the FM QCP further experiments are required, like transport measurement for various directions of the magnetic fields and specific-heat measurements for $B \parallel a$ and $B \parallel b$. Finally, we recall that $URh_{0.62}Ru_{0.38}Ge$ is one of the scarce materials at a FM QCP at ambient pressure, and thus offers a unique testing ground for the study of critical ferromagnetic spin fluctuations by microscopic techniques, like inelastic neutron scattering or NMR.